IEEE Access
Multidisciplinary : Rapid Review : Open Access Journal

Received September 12, 2017, accepted October 6, 2017, date of publication October 10, 2017, date of current version November 14, 2017.

Digital Object Identifier 10.1109/ACCESS.2017.2761845

Space-Time Multiple-Mode Orthogonal Frequency Division Multiplexing With Index Modulation

JUN LI[1,2], (Member, IEEE), MIAOWEN WEN[2,3], (Member, IEEE), XUEQIN JIANG[4], (Member, IEEE), AND WEI DUAN[5]

[1]School of Mechanical and Electrical Engineering, Guangzhou University, Guangzhou 510006, China
[2]National Mobile Communications Research Laboratory, Southeast University, Nanjing 210096, China
[3]School of Electronic and Information Engineering, South China University of Technology, Guangzhou 510641, China
[4]School of Information Science and Technology, Donghua University, Shanghai 201620, China
[5]School of Electronics and Information, Nantong University, Nantong 226019, China

Corresponding author: Miaowen Wen (eemwwen@scut.edu.cn)

This work was supported in part by the National Nature Science Foundation of China under Grant 61701127, Grant 61501190, and Grant 61671143, in part by the Guangzhou University Project under Grant 2700050338, in part the Guangzhou City Science and Technology Project under Grant 201605030014, and in part by the open research fund of National Mobile Communications Research Laboratory, Southeast University under Grant 2017D08.

ABSTRACT Multiple-mode orthogonal frequency division multiplexing with index modulation (MM-OFDM-IM) improves the spectral efficiency of the conventional OFDM-IM scheme by considering multiple distinguishable constellations for signal modulation. In this paper, we propose a novel scheme, called space-time MM-OFDM-IM (ST-MM-OFDM-IM), to increase the transmit diversity of MM-OFDM-IM. In ST-MM-OFDM-IM, the signal matrix, which consists of multiple signal vectors of MM-OFDM-IM, is transmitted over multiple time slots by following a specific rule. A low-complexity detection is proposed to mitigate the high burden of the optimal maximum-likelihood detection at the receiver side. A closed-form upper bound on the bit error rate is derived to evaluate the performance of ST-MM-OFDM-IM. Moreover, a diversity improving scheme of ST-MM-OFDM-IM is also studied to obtain full transmit diversity. Simulation results verify the theoretical analysis and show that ST-MM-OFDM-IM outperforms the conventional MM-OFDM-IM scheme.

INDEX TERMS Space-time domain, OFDM, index modulation, bit error rate.

I. INTRODUCTION

Index modulation (IM) technique makes good use of the index(es) of transmission media, such as transmit or receive antennas, subcarriers, time slots or linear block codes, to modulate information bits by some mapping rules [1], [2]. Since the transmission of index(es) produces very less or even no power consumption, IM exploits a feasible trade-off between the spectral efficiency (SE) and energy efficiency (EE), or the diversity gain and multiplexing gain, which has the great potential for green communications in the future fifth generation (5G) networks.

Spatial modulation (SM), which first applies the IM concept into the space domain, can be considered as a special case of multi-input-multi-output (MIMO) techniques [3]–[6]. In SM, the information bits are comprised of the index bits and modulation bits. The index bits are conveyed via the index of a single active antenna, and the modulation bits are mapped to a modulation symbol transmitted by the active antenna. Many advantages of SM exist, such as the high EE and free inter-channel interference (ICI). To further simplify the SM system, space shift keying (SSK) is proposed to transmit only the index of the active transmit antenna [7]. However, the critical deficiency is that the SE of SM or SSK is much lower than that of the conventional MIMO system. To overcome this problem, plenty of studies have been done to increase the SE of SM and SSK [8]–[10]. In [8], generalized SM (GSM) is proposed to increase the SE of SM by activating more than one transmit antennas. Similarly, to improve the SE of SSK, generalized SSK (GSSK) is also proposed to transmit information bits through the indices of multiple transmit antennas [9]. Quadrature SM (QSM) is designed to double the index bits of SM by expanding the modulated symbol into in-phase and quadrature domains in [10] and [11]. In addition, extending SM into space-time (ST) domain, such as space-time shift keying (STSK), space-time block coded SM (STBC-SM) and time-indexed SM (TI-SM), has been proposed to improve the transmit diversity or performance of SSK and SM, respectively [12]–[14]. Moreover, differential SM (DSM) [15], [16], which is also an ST domain extension of SM, is proposed to transmit the additional index bits via antenna activation permutations without the need of the channel state information at the receiver side. On the other hand, a new SM scheme, called receive SM (RSM) or pre-coding SM (PSM), has been developed in [17], which coveys the index bits via the index of a single receive antenna. By utilizing the pre-coding techniques, such as zero-forcing (ZF) or minimum mean square error (MMSE) per-coding methods, PSM acquires better performance than the conventional SM scheme. Due to this benefit, many related works have been proposed [18]–[20]. In [18], generalised PSM (GPSM) is proposed to activate more than one receive antennas in PSM. GPSM expanded to the multi-stream system is studied in [19]. In addition, an extension of GPSM into the in-phase and quadrature domains is proposed in [20], which further increases the SE of GPSM largely.

Recently, the IM concept is also applied into the frequency domain, which is incorporated in orthogonal frequency division multiplexing (OFDM) systems. Subcarrier-index modulation OFDM (SIM-OFDM) [21] is first proposed to transmit index bits by OFDM subcarriers, which is subject to the error propagation effect. To mitigate this problem, enhanced SIM-OFDM (ESIM-OFDM) is then proposed to use one index bit to control two consecutive subcarriers, which activates only one subcarrier in each subcarrier pair [22]. However, compared to the conventional OFDM, SIM-OFDM or ESIM-OFDM has a much smaller SE, especially for a high-order modulation scheme. Therefore, a flexible IM scheme, called OFDM with IM (OFDM-IM), is proposed in [23], which transmits several index bits via multiple subcarriers. In OFDM-IM, a subset of subcarriers are activated to transmit modulated symbols and the additional index bits are conveyed by the indices of the active subcarriers or the subcarrier activation pattern (SAP). Obviously, some remaining subcarriers are inactive. The index bits can be determined by different mapping methods of SAPs, such as the combinatorial method [23] or the equiprobable subcarrier activation method [24]. In [23], it can be seen that the OFDM-IM scheme is shown to achieve better bit error rate (BER) performance than the conventional OFDM scheme under the same SE. Attracted by this advantage, many related works have been investigated. The interleaved subcarrier grouping method is applied to improve the BER performance of OFDM-IM without any additional resource [25], [26]. The optimal subcarrier activation method is studied by maximizing the achievable rate in [26]. Another subcarrier activation method is designed to maximize the minimum Euclidean distance of receive vectors in [27]. It is worth noting that not all SAPs are used to map the index bits in above-mentioned literature, which leads to performance degradation of OFDM-IM. Therefore, the authors in [28] map all SAPs into the index bits by resorting to a specific constellation order. To further improve the transmit diversity of OFDM-IM, the coordinated interleaving OFDM-IM is proposed in [29], which attains the transmit diversity order of two. Additionally, the OFDM-IM is applied into some practical situations, such as the underwater acoustic communications [30] and visible light communications [31].

In order to increase the SE of OFDM-IM, more extensions of OFDM-IM have appeared in the literature. In [32], OFDM with generalized index modulation (OFDM-GIM) and OFDM with in-phase/quadrature index modulation (OFDM-I/Q-IM) are both proposed to increase the length of index bits of OFDM-IM. Besides, to linearly increase the SE of OFDM-IM, MIMO-OFDM-IM is proposed by merging the MIMO and OFDM-IM schemes together [33]. The low-complexity detection methods for OFDM-IM and MIMO-OFDM-IM are depicted in [34]–[36]. It is worth noting that, the inactive subcarriers in all above literature do not carry any information. However, based on the basic concept of OFDM-IM, the (generalized-)dual-mode IM aided OFDM ((G-)DM-OFDM) in in [37] and [38] is cleverly developed by conveying the additional modulated symbols through the inactive subcarriers. In [39], multiple-mode OFDM-IM (MM-OFDM-IM) is proposed to transmit the modulated symbols by all subcarriers and to use the permutations of different constellation sets to carry index bits.

Motivated by STSK and MM-OFDM-IM, we propose a novel IM scheme, namely ST-MM-OFDM-IM, to increase the transmit diversity or equivalently improve the BER performance of MM-OFDM-IM. Unlike the transmission over a single time slot in MM-OFDM-IM, ST-MM-OFDM-IM transmits a signal matrix over n time slots by following a certain subcarrier activation rule, where n denotes the length of the OFDM subblock. For ease of implementation, a low-complexity detection method is also designed to combat the high computational complexity of the optimal maximum-likelihood (ML) detection. We then study the BER performance of ST-MM-OFDM-IM under the Rayleigh fading channels. Specifically, we derive an upper bound on the BER by the union bounding technique and characterize the diversity order of ST-MM-OFDM-IM. In addition, a diversity improvement scheme of ST-MM-OFDM-IM is further proposed to improve the transmit diversity up to n by appropriately selecting some subcarrier activation matrices or index matrices. Computer simulations are conducted to investigate the performance of ST-MM-OFDM-IM. Simulation results show that the ST-MM-OFDM-IM scheme achieves a transmit diversity of two, which significantly reduces the BER of MM-OFDM-IM. It is also shown that the diversity improvement scheme of ST-MM-OFDM-IM indeed obtains a diversity order of n.

The rest of this paper is organized as follows. In Section II, we introduce the system model of the MM-OFDM-IM

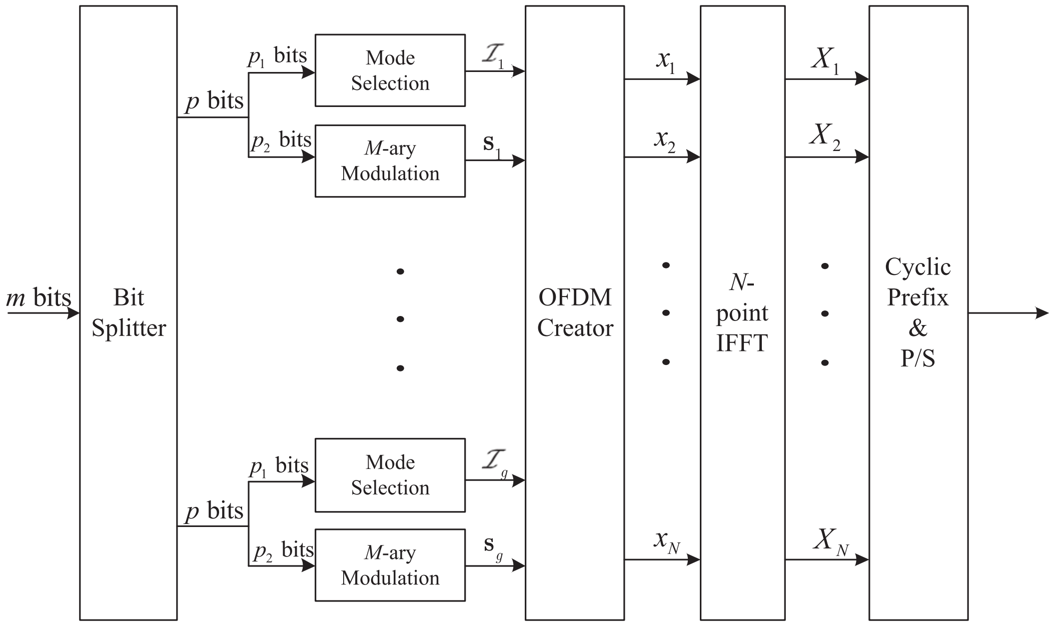

FIGURE 1. System model for MM-OFDM-IM.

schemes. The principle and the low-complexity detection for the ST-MM-OFDM-IM scheme are clarified in Section III. Section IV presents the upper bound on the BER and the diversity improving scheme for the ST-MM-OFDM-IM scheme. Simulation results are discussed in Section V. Finally, this paper is concluded in Section VI.

Notations: Upper and lower case boldface letters denote matrices and column vectors, respectively. The complex number field is represented by $\mathbb{C}$. $(\cdot)^T$ and $(\cdot)^H$ and represent the transpose and Hermitian transpose operations, respectively. $\mathbf{I}_M$ is an identity matrix of size $M \times M$. $||\cdot||$ and $C(\cdot,\cdot)$ denote the Frobenius norm and binomial operations, respectively. $Q(\cdot)$ and rank$\{\cdot\}$ represent the Gaussian Q-function [40] and the rank of the argument, respectively. diag$\{\mathbf{x}\}$ denotes a diagonal matrix whose diagonal elements are drawn from $\mathbf{x}$. $X \sim \mathcal{CN}(0, \delta^2)$ represents the distribution of a circularly symmetric complex Gaussian r.v. X with variance δ^2. The probability of an event is denoted by Pr$(\cdot)$. $\lfloor \cdot \rfloor$ indicates the floor operations.

II. OVERVIEW OF MM-OFDM-IM

We introduce the MM-OFDM-IM scheme in Fig. 1, which increases the SE of OFDM-IM by activating all subcarriers [39]. The total N OFDM subcarriers are divided into g groups, each group consisting of n subcarriers with $n = N/g$. The information bits of length m are split into g blocks, each containing $p = m/g$ bits. For each block, p bits are separated into two parts: p_1 and p_2 bits. Take the α-th block for example, where $\alpha \in \{1, 2, \ldots, g\}$. The first part of p_1 bits is used to select the order of constellation modes $\{\mathcal{S}_{i_{\alpha,1}}, \ldots, \mathcal{S}_{i_{\alpha,n}}\}$ corresponding to n subcarriers, where $\mathcal{S}_{i_{\alpha,\tau}}$ with $\tau = 1, 2, \ldots, n$ and $i_{\alpha,\tau} \in \{1, 2, \ldots, n\}$ is the M-ary constellation that is distinguishable from the other $(n-1)$ constellations. The corresponding permutation indices for $\{\mathcal{S}_{i_{\alpha,\tau}}\}_{\tau=1}^n$ are given by

TABLE 1. Mapping table for MM-OFDM-IM with $n = 3$ and $p_1 = 2$.

p_1 bits	$\mathcal{I}_\alpha$	constellation modes
[0,0]	$\{1,2,3\}$	$\mathcal{S}_1, \mathcal{S}_2, \mathcal{S}_3$
[0,1]	$\{1,3,2\}$	$\mathcal{S}_1, \mathcal{S}_3, \mathcal{S}_2$
[1,0]	$\{2,1,3\}$	$\mathcal{S}_2, \mathcal{S}_1, \mathcal{S}_3$
[1,1]	$\{2,3,1\}$	$\mathcal{S}_2, \mathcal{S}_3, \mathcal{S}_1$

$$\mathcal{I}_\alpha = \{i_{\alpha,1}, \ldots, i_{\alpha,n}\}. \tag{1}$$

Note that there are $n!$ permutation sets for $\{\mathcal{S}_{i_{\alpha,\tau}}\}_{\tau=1}^n$, which leads to $p_1 = \lfloor \log_2(n!) \rfloor$. The mapping method of the p_1 bits to the permutation set can be directly obtained by the look-up table or combinatorial method in [39]. An example of permutation indices with $n = 3$ and $p_1 = 2$ is given in Table 1. The second part of p_2 bits is used to determine the modulated symbol set

$$\mathbf{s}_\alpha = \{s_{\alpha,1}, \ldots, s_{\alpha,n}\}, \tag{2}$$

which are transmitted through the selected constellation modes $\{\mathcal{S}_{i_{\alpha,\tau}}\}_{\tau=1}^n$. It is obvious that $p_2 = n\log_2(M)$.

After obtaining $s_{\alpha,\tau}$ for all α and τ, the OFDM symbol vector in the frequency-domain can be expressed by

$$\begin{aligned}\mathbf{x} &= [x_1, \ldots, x_N]^T \\ &= \left[s_{1,1}, s_{1,2}, \ldots, s_{1,n}, \ldots, s_{g,1}, s_{g,2}, \ldots, s_{g,n}\right]^T.\end{aligned} \tag{3}$$

The following procedure is the same as the conventional OFDM scheme. Applying the N-point inverse fast

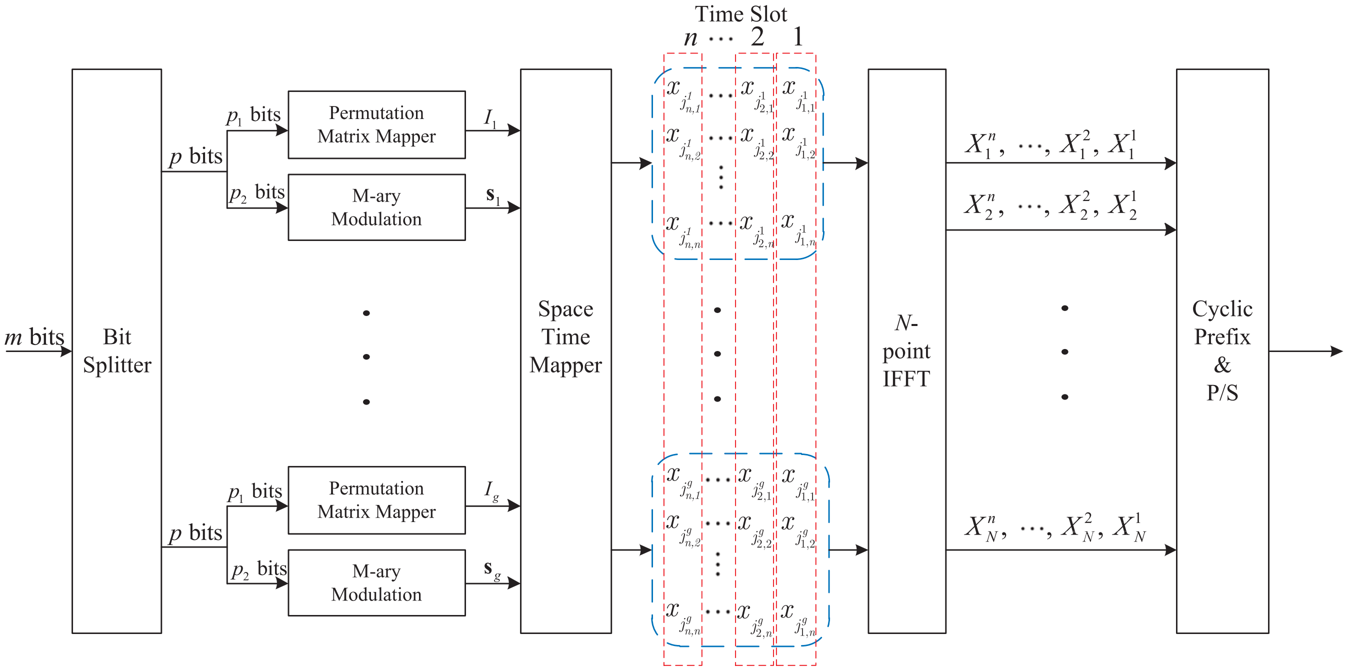

FIGURE 2. System model for STMM-OFDM-IM.

Fourier transform (IFFT) to the OFDM symbol vector $\mathbf{x}$, we obtain the time-domain OFDM symbol vector $\mathbf{x}_t = [X_1, X_2, \ldots, X_N]^T$. Then, after appending the cyclic prefix (CP) to the beginning of $\mathbf{x}_t$ and parallel to serial (P/S) conversion, the OFDM signal is transmitted.

At the receiver side, the frequency-domain signal is obtained by removing CP and applying FFT

$$\bar{y}_\gamma = \bar{h}_\gamma x_\gamma + \bar{w}_\gamma, \quad \gamma = 1, 2, \ldots, N, \tag{4}$$

where $\bar{h}_\gamma$ and $\bar{w}_\gamma$ are the channel coefficient and the additive white Gaussian noise (AWGN) at the γ-th subcarrier which are distributed as $\mathcal{CN}(0, 1)$ and $\mathcal{CN}(0, N_0)$, respectively. The SE of MM-OFDM-IM without considering the CP is

$$SE_{\text{MM-OFDM-IM}} = \frac{p_1 + p_2}{n} = \frac{\lfloor \log_2(n!) \rfloor}{n} + \log_2(M). \tag{5}$$

Since all groups in the OFDM block are independent of each other, the detection of the permutation indices (or constellation modes) and modulated symbols can be implemented group by group through the optimal ML detection, which can be represented by

$$\left(\hat{\mathcal{I}}_\alpha, \hat{\mathbf{s}}_\alpha\right) = \arg\min_{\mathcal{I}_\alpha, \mathbf{s}_\alpha} \sum_{\varsigma=1}^{n} |\bar{y}(\alpha, \varsigma) - \bar{h}(\alpha, \varsigma) s_{\alpha,\varsigma}|^2, \tag{6}$$

where $\bar{y}(\alpha, \varsigma) = \bar{y}_{(\alpha-1)n+\varsigma}$ and $\bar{h}(\alpha, \varsigma) = \bar{h}_{(\alpha-1)n+\varsigma}$. From (6), it can be seen that the optimal ML detection requires a high computational complexity of order $\sim \mathcal{O}(n!M^n)$ when n or M is a large value. To figure out this problem, some low-complexity detection methods are proposed to achieve the near-ML/near-optimal performance (Refer to [39] for more details). After obtaining the constellation modes and modulated symbols, total m information bits can be directly recovered by the mode demapper and the signal demodulator.

III. PROPOSED ST-MM-OFDM-IM

In this section, to increase the diversity order of MM-OFDM-IM systems, we propose a novel scheme, namely ST-MM-OFDM-IM, which extends the MM concept into both space domain and time domain.

Fig. 2 shows the system model of ST-MM-OFDM-IM. In ST-MM-OFDM-IM, the OFDM block corresponding to N subcarriers are divided into g groups while each group consists of n subcarriers with $n = N/g$. The m bits are also split into g groups and p bits are allocated for each group with $m = pg$. Since all groups are independent, we only take into account the α-th group with p bits and n subcarriers for analysis. The p bits are also divided into p_1 and p_2 bits. The first part of p_1 bits, namely index bits, determines the order of the MM matrix, which consists of multiple constellation modes over n time slots and can be expressed as

$$\begin{bmatrix} \mathcal{S}_{j^\alpha_{1,1}} & \mathcal{S}_{j^\alpha_{2,1}} & \cdots & \mathcal{S}_{j^\alpha_{n,1}} \\ \mathcal{S}_{j^\alpha_{1,2}} & \mathcal{S}_{j^\alpha_{2,2}} & \cdots & \mathcal{S}_{j^\alpha_{n,2}} \\ \vdots & \vdots & \ddots & \vdots \\ \mathcal{S}_{j^\alpha_{1,n}} & \mathcal{S}_{j^\alpha_{2,n}} & \cdots & \mathcal{S}_{j^\alpha_{n,n}} \end{bmatrix}, \tag{7}$$

where $j^\alpha_{\mu,\tau} \in \{1, 2, \ldots, n\}$ denotes the mode index at the μ-th time slot with $\mu, \tau \in \{1, 2, \ldots, n]\}$. $\mathcal{S}_{j^\alpha_{\mu,\tau}}$ represents the M-ary constellation, which as similar to MM-OFDM-IM that is distinguishable from each other at the μ-th time slot. The

TABLE 2. Mapping table for ST-MM-OFDM-IM with $n = 2$ and $p_1 = 2$.

p_1 bits	$\mathcal{J}_\alpha$	MM matrix
0	$\begin{bmatrix} 1 & 2 \\ 2 & 1 \end{bmatrix}$	$\begin{bmatrix} \mathcal{S}_1 & \mathcal{S}_2 \\ \mathcal{S}_2 & \mathcal{S}_1 \end{bmatrix}$
1	$\begin{bmatrix} 2 & 1 \\ 1 & 2 \end{bmatrix}$	$\begin{bmatrix} \mathcal{S}_2 & \mathcal{S}_1 \\ \mathcal{S}_1 & \mathcal{S}_2 \end{bmatrix}$

TABLE 3. The number of Latin squares with varying n.

n	Number of Latin squares	Representative example
1	$L_1 = 1$	[1]
2	$L_2 = 2$	$\begin{bmatrix} 1 & 2 \\ 2 & 1 \end{bmatrix}$
3	$L_3 = 12$	$\begin{bmatrix} 1 & 3 & 2 \\ 2 & 1 & 3 \\ 3 & 2 & 1 \end{bmatrix}$
4	$L_4 = 576$	$\begin{bmatrix} 1 & 3 & 2 & 4 \\ 2 & 1 & 4 & 3 \\ 3 & 4 & 1 & 2 \\ 4 & 2 & 3 & 1 \end{bmatrix}$
5	$L_5 = 161280$	$\begin{bmatrix} 1 & 5 & 3 & 2 & 4 \\ 2 & 1 & 4 & 3 & 5 \\ 3 & 2 & 5 & 4 & 1 \\ 4 & 3 & 1 & 5 & 2 \\ 5 & 4 & 2 & 1 & 3 \end{bmatrix}$

corresponding index matrix of the MM matrix is given by

$$\mathcal{J}_\alpha = \begin{bmatrix} j_{1,1}^\alpha & j_{2,1}^\alpha & \cdots & j_{n,1}^\alpha \\ j_{1,2}^\alpha & j_{2,2}^\alpha & \cdots & j_{n,2}^\alpha \\ \vdots & \vdots & \ddots & \vdots \\ j_{1,n}^\alpha & j_{2,n}^\alpha & \cdots & j_{n,n}^\alpha \end{bmatrix}. \tag{8}$$

It is worth noting that the indices in each column (each time slot) should be all different to satisfy the MM-OFDM-IM concept in the proposed scheme. However, in order to achieve the diversity improvement, our scheme also requires the indices in each row to be different from each other. An example of a mapping table for $n = 2$ and $p_1 = 2$ is given in Table 2. In this example, we can see that the elements in all MM matrices and the corresponding index matrices occur exactly once in each row and each column, which satisfies the property of the well known Latin square [41]. The example of Latin squares with $n = 1, \ldots, 5$ is shown in Table 3, where L_n denotes the number of Latin squares. To modulate the p_1 bits, we only need $2^{\lfloor \log_2(L_n) \rfloor}$ Latin squares as the legal realizations with $p_1 = \lfloor \log_2(L_n) \rfloor$. In this paper, we briefly map the p_1 bits to the index matrix $\mathcal{J}_\alpha$ by the look-up table method (also see the mapping table for $n = 3$ and $p_1 = 3$ in Table 4). The second part of p_2 bits, namely modulation bits, are used to generate n modulated symbols $\mathbf{s}_\alpha = \{s_{\alpha,1}, \ldots, s_{\alpha,n}\}$ with $p_2 = n \log_2(M)$, which are transmitted over n subcarriers at all time slots. Note that at each time slot, the same modulated symbols are transmitted by following the constellation modes in $\mathcal{J}_\alpha$.

TABLE 4. Mapping table for ST-MM-OFDM-IM with $n = 3$ and $p_1 = 3$.

p_1 bits	$\mathcal{J}_\alpha$	MM matrix
$[0,0,0]$	$\begin{bmatrix} 1 & 2 & 3 \\ 2 & 3 & 1 \\ 3 & 1 & 2 \end{bmatrix}$	$\begin{bmatrix} \mathcal{S}_1 & \mathcal{S}_2 & \mathcal{S}_3 \\ \mathcal{S}_2 & \mathcal{S}_3 & \mathcal{S}_1 \\ \mathcal{S}_3 & \mathcal{S}_1 & \mathcal{S}_2 \end{bmatrix}$
$[0,0,1]$	$\begin{bmatrix} 1 & 3 & 2 \\ 2 & 1 & 3 \\ 3 & 2 & 1 \end{bmatrix}$	$\begin{bmatrix} \mathcal{S}_1 & \mathcal{S}_3 & \mathcal{S}_2 \\ \mathcal{S}_2 & \mathcal{S}_1 & \mathcal{S}_3 \\ \mathcal{S}_3 & \mathcal{S}_2 & \mathcal{S}_1 \end{bmatrix}$
$[0,1,0]$	$\begin{bmatrix} 1 & 2 & 3 \\ 3 & 1 & 2 \\ 2 & 3 & 1 \end{bmatrix}$	$\begin{bmatrix} \mathcal{S}_1 & \mathcal{S}_2 & \mathcal{S}_3 \\ \mathcal{S}_3 & \mathcal{S}_1 & \mathcal{S}_2 \\ \mathcal{S}_2 & \mathcal{S}_3 & \mathcal{S}_1 \end{bmatrix}$
$[0,1,1]$	$\begin{bmatrix} 1 & 3 & 2 \\ 3 & 2 & 1 \\ 2 & 1 & 3 \end{bmatrix}$	$\begin{bmatrix} \mathcal{S}_1 & \mathcal{S}_3 & \mathcal{S}_2 \\ \mathcal{S}_3 & \mathcal{S}_2 & \mathcal{S}_1 \\ \mathcal{S}_2 & \mathcal{S}_1 & \mathcal{S}_3 \end{bmatrix}$
$[1,0,0]$	$\begin{bmatrix} 2 & 1 & 3 \\ 1 & 3 & 2 \\ 3 & 2 & 1 \end{bmatrix}$	$\begin{bmatrix} \mathcal{S}_2 & \mathcal{S}_1 & \mathcal{S}_3 \\ \mathcal{S}_1 & \mathcal{S}_3 & \mathcal{S}_2 \\ \mathcal{S}_3 & \mathcal{S}_2 & \mathcal{S}_1 \end{bmatrix}$
$[1,0,1]$	$\begin{bmatrix} 2 & 3 & 1 \\ 1 & 2 & 3 \\ 3 & 1 & 2 \end{bmatrix}$	$\begin{bmatrix} \mathcal{S}_2 & \mathcal{S}_3 & \mathcal{S}_1 \\ \mathcal{S}_1 & \mathcal{S}_2 & \mathcal{S}_3 \\ \mathcal{S}_3 & \mathcal{S}_1 & \mathcal{S}_2 \end{bmatrix}$
$[1,1,0]$	$\begin{bmatrix} 2 & 1 & 3 \\ 3 & 2 & 1 \\ 1 & 3 & 2 \end{bmatrix}$	$\begin{bmatrix} \mathcal{S}_2 & \mathcal{S}_1 & \mathcal{S}_3 \\ \mathcal{S}_3 & \mathcal{S}_2 & \mathcal{S}_1 \\ \mathcal{S}_1 & \mathcal{S}_3 & \mathcal{S}_2 \end{bmatrix}$
$[1,1,1]$	$\begin{bmatrix} 2 & 3 & 1 \\ 3 & 1 & 2 \\ 1 & 2 & 3 \end{bmatrix}$	$\begin{bmatrix} \mathcal{S}_2 & \mathcal{S}_3 & \mathcal{S}_1 \\ \mathcal{S}_3 & \mathcal{S}_1 & \mathcal{S}_2 \\ \mathcal{S}_1 & \mathcal{S}_2 & \mathcal{S}_3 \end{bmatrix}$

According to $\mathcal{J}_\alpha$ (or MM matrix) and $\mathbf{s}_\alpha$, the transmitted matrix is given by

$$\mathbf{X}_\alpha = \begin{bmatrix} x_{j_{1,1}^\alpha} & x_{j_{2,1}^\alpha} & \cdots & x_{j_{n,1}^\alpha} \\ x_{j_{1,2}^\alpha} & x_{j_{2,2}^\alpha} & \cdots & x_{j_{n,2}^\alpha} \\ \vdots & \vdots & \ddots & \vdots \\ x_{j_{1,n}^\alpha} & x_{j_{2,n}^\alpha} & \cdots & x_{j_{n,n}^\alpha} \end{bmatrix}. \tag{9}$$

After obtaining $\{\mathbf{X}_\alpha\}_{\alpha=1}^{g}$, the $N \times n$ OFDM block matrix over n time slots in the frequency-domain is given by

$$\mathbf{X} = [\mathbf{X}_1^T, \mathbf{X}_2^T, \ldots, \mathbf{X}_g^T]^T. \tag{10}$$

Applying the N-point IFFT to $\mathbf{X}_\alpha$, we obtain the time domain OFDM block matrix $\tilde{\mathbf{X}} = [\mathbf{x}_T(1), \mathbf{x}_T(2), \ldots, \mathbf{x}_T(N)]^T$, where $\mathbf{x}_T(\gamma) = [X_\gamma^1, X_\gamma^2, \ldots, X_\gamma^n]^T$ with $\gamma \in \{1, 2, \ldots, N\}$. Finally, after the CP appending and the P/S conversion, the signal matrix is transmitted through a slowly time-varying Rayleigh fading channel over n time slots. Assume that the channel coefficients, which can be characterized as

$$\tilde{\mathbf{h}} = [\tilde{h}_1, \tilde{h}_2, \ldots, \tilde{h}_\rho], \tag{11}$$

where ρ represents the number of channel taps, and $\tilde{h}_\varrho \sim \mathcal{CN}(0, 1/\rho)$ with $\varrho = 1, 2, \ldots, \rho$ remains constant over n time slots. At the receiver side, by removing the CP from the received signal matrix and applying the

N-point FFT, the frequency-domain signal matrix is obtained as

$$\mathbf{Y} = \mathbf{H}\mathbf{X} + \mathbf{W}, \tag{12}$$

where $\mathbf{H} = \text{diag}\{\mathbf{h}\}$, $\mathbf{h} = [h_1, h_2, \dots, h_N]^T$ is the $N \times 1$ frequency-domain channel coefficients with $\mathcal{CN}(0, \mathbf{I}_N)$ and $\mathbf{W}$ is the frequency-domain noise matrix with $\mathcal{CN}(0, N_0\mathbf{I}_N)$. By dispensing with CP, the SE of ST-MM-OFDM-IM can be calculated by

$$\begin{aligned} SE_{\text{ST-MM-OFDM-IM}} &= \frac{p_1 + p_2}{n^2} \\ &= \frac{\lfloor \log_2(L_n) \rfloor + n\log_2(M)}{n^2}. \end{aligned} \tag{13}$$

Due to the independence between all groups, the detection of the index matrix and modulated symbols can be performed group by group. Therefore, we only consider the detection for the α-th group by the optimal ML detection

$$\left(\hat{\mathcal{J}}_\alpha, \hat{\mathbf{s}}_\alpha\right) = \arg\min_{\mathcal{J}_\alpha, \mathbf{s}_\alpha} \|\mathbf{Y}_\alpha - \mathbf{H}_\alpha \mathbf{X}_\alpha\|^2, \tag{14}$$

where $\mathbf{H}_\alpha = \text{diag}\{\mathbf{h}_\alpha\}$, $\mathbf{h}_\alpha$ is the sub-vector of $\mathbf{h}$ corresponding to the α-th group, and $\mathbf{Y}_\alpha$ is the sub-matrix of $\mathbf{Y}$ corresponding to the α-th group.

From (14), we see that the computational complexity of the optimal ML detection is of order $\sim \mathcal{O}(L_n M^n)$. As shown in Table 3, it can be found that the number of Latin squares L_n with $n > 4$ is too large, which is impractical for the optimal ML detection. Therefore, in the following, we propose a low-complexity detection to solve this problem. To begin with, we express all possible row modes corresponding to the elements of each row in the index matrix as

$$\begin{aligned} \Theta_n &= \{\Theta_n(1), \Theta_n(2), \dots, \Theta_n(n!)\} \\ &= \{[1, 2, \dots, n], [2, 1, \dots, n], \quad \cdots, [n, n-1, \dots, 1]\}. \end{aligned} \tag{15}$$

Obviously, there are $n!$ realizations for Θ_n. For example, if $n = 3$, we have

$$\begin{aligned} \Theta_3 &= \{\Theta_n(1), \Theta_n(2), \Theta_n(3), \Theta_n(4), \Theta_n(5), \Theta_n(6)\} \\ &= \{[1, 2, 3], [1, 3, 2], [2, 1, 3], [2, 3, 1], [3, 1, 2], \\ &\qquad [3, 2, 1]\}. \end{aligned} \tag{16}$$

Alternatively, the set of row modes with $n = 4$ is given as follows

$$\begin{aligned} \Theta_4 &= \{\Theta_n(1), \Theta_n(2), \dots, \Theta_n(24)\} \\ &= \{[1, 2, 3, 4], [1, 2, 4, 3], \dots, [4, 3, 1, 2], [4, 3, 2, 1]\}. \end{aligned} \tag{17}$$

Note that all rows of the index matrix (all row modes) are selected from Θ_n by following the rule of Latin square. Accordingly, we may search each row mode from Θ_n individually rather than search the entire 2^{p_1} possible candidates of index matrices in the optimal ML detection, which largely reduces the computational complexity. The proposed low-complexity detection operates as follows:

- Sort the channel coefficients in $\mathbf{h}_\alpha$ in a descending order: $|h_{q_1}|^2 > |h_{q_2}|^2 > \cdots > |h_{q_n}|^2 (|h_{q_1}| > |h_{q_2}| > \cdots > |h_{q_n}|)$ with $q_\tau, \tau \in [1, 2, \dots, n]$. Note that h_{q_1} is the strongest channel and h_{q_n} is the weakest channel for all n subcarriers.
- Detect the row mode from the strongest channel h_{q_1} to the weakest channel h_{q_n} by following the order of $\{q_1, q_2, \dots, q_n\}$. Specifically, we first determine the row mode and the modulated symbols at the q_1-th subcarrier (corresponding to the strongest channel) by calculating the Euclidean distance
$$\left(\hat{\mathcal{J}}_\alpha(q_1), \hat{\mathbf{s}}_\alpha\right) = \arg\min_{\mathcal{J}_\alpha(q_1) \in \Theta_n, \mathbf{s}_\alpha} \|\mathbf{Y}_\alpha(q_1) - h_{q_1}\mathbf{X}_\alpha(q_1)\|^2, \tag{18}$$
where $\mathcal{J}_\alpha(q_1)$, $\mathbf{X}_\alpha(q_1)$ and $\mathbf{Y}_\alpha(q_1)$ denote the q_1-th row of $\mathcal{J}_\alpha$, $\mathbf{X}_\alpha$ and $\mathbf{Y}_\alpha$, respectively.
- Find the illegal row modes $\{\mathbf{r}_1, \dots, \mathbf{r}_\iota\}$ in the light of $\hat{\mathcal{J}}_\alpha(q_1)$, where ι is the number of illegal row modes in Θ_n. Then, we delete the illegal row modes including $\hat{\mathcal{J}}_\alpha(q_1)$ from Θ_n to generate an updated row mode set Θ'_n. Note that as the modulated symbols have been already estimated in the second step, we only need to detect the row mode for the q_2-th subcarrier by
$$\left(\hat{\mathcal{J}}_\alpha(q_2)\right) = \arg\min_{\mathcal{J}_\alpha(q_2) \in \Theta'_n} \|\mathbf{Y}_\alpha(q_2) - h_{q_2}\mathbf{X}_\alpha(q_2)\|^2. \tag{19}$$
- Until the row mode at the q_n-th subcarrier is obtained, then the final index matrix $\mathcal{J}_\alpha$ as well as the estimated modulated symbols are set as the outputs.

The procedure of the proposed low-complexity detection with $n = 3$ is exemplified in Fig. 3. From Fig. 3, it can be seen that the channels are sorted as $|h_2| > |h_1| > |h_3|$ and the row mode [1 3 2] is first estimated with red color (red tick) from Θ_3 for the second subcarrier (h_2) in Step 1. Note that the modulated symbols are also estimated but not shown for brevity. After setting $\mathcal{J}_\alpha(2) = [1\ 3\ 2]$, three row modes [1 2 3], [2 3 1] and [3 1 2] are excluded with green color (green cross) from Θ_3 and the updated set Θ'_3 composes of the remaining row modes [2 1 3] and [3 2 1] with blue color (blue circle). In Step 2, the row mode [2 1 3] is then estimated with red color for the first subcarrier (h_1) and we have $\mathcal{J}_\alpha(1) = [2\ 1\ 3]$. Apparently, the last remaining row mode [3 2 1] is allocated for the third subcarrier (h_3), which leads to $\mathcal{J}_\alpha(3) = [3\ 2\ 1]$. Finally, we get the index matrix

$$\mathcal{J}_\alpha = \begin{bmatrix} 2 & 1 & 3 \\ 1 & 3 & 2 \\ 3 & 2 & 1 \end{bmatrix}. \tag{20}$$

The information bits can be easily recovered by the demapping of the index matrix and demodulation of the modulated symbols.

IV. PERFORMANCE ANALYSIS AND DIVERSITY IMPROVING SCHEME

In this section, an upper bound on the BER is derived and a diversity improving scheme is propsoed.

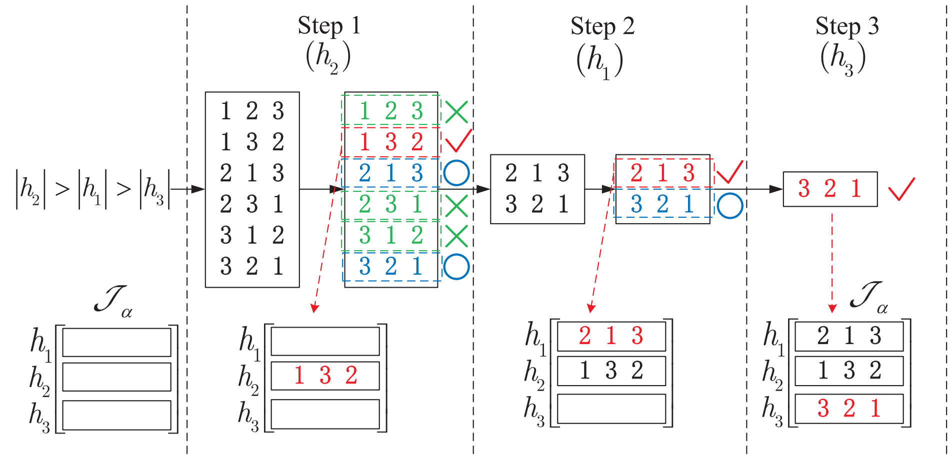

FIGURE 3. Illustration of the low-complexity detection with $n = 3$.

A. UPPER BOUND ANALYSIS

In this subsection, we analytically derive the upper bound on the BER of ST-MM-OFDM-IM. For ease of analysis, we will omit the notation α in the following. In light of (14), the conditional pairwise error probability (PEP) of detecting $\hat{\mathbf{X}}$ when $\mathbf{X}$ is transmitted on $\mathbf{H}$ can be calculated as

$$\begin{aligned}\Pr\left\{\mathbf{X}\to\hat{\mathbf{X}}\,|\mathbf{H}\right\} &= \Pr\left\{\|\mathbf{Y}-\mathbf{H}\mathbf{X}\|_F^2 > \left\|\mathbf{Y}-\mathbf{H}\hat{\mathbf{X}}\right\|_F^2\right\}\\ &= \Pr\left\{\sum_{i=1}^{n}\|\mathbf{y}_i-\mathrm{diag}\{\mathbf{x}_i\}\mathbf{h}\|^2 > \sum_{i=1}^{n}\|\mathbf{y}_i-\mathrm{diag}\left\{\hat{\mathbf{x}}_i\right\}\mathbf{h}\|^2\right\}\\ &= Q\left(\sqrt{\frac{\sum_{i=1}^{n}\|\mathrm{diag}\left\{\mathbf{x}_i-\hat{\mathbf{x}}_i\right\}\mathbf{h}\|^2}{2N_0}}\right),\end{aligned} \tag{21}$$

where $\mathbf{y}_i$, $\mathbf{x}_i$ and $\hat{\mathbf{x}}_i$ represent the i-th column of $\mathbf{Y}$, $\mathbf{X}$ and $\hat{\mathbf{X}}$, respectively.

Applying the Q-function approximation [42]

$$Q(x) \cong \frac{1}{12}e^{-\frac{x^2}{2}} + \frac{1}{4}e^{-\frac{2x^2}{3}}, \tag{22}$$

the unconditional PEP can be approximated as [23]

$$\begin{aligned}\Pr\left\{\mathbf{X}\to\hat{\mathbf{X}}\right\} &= E_{\mathbf{h}}\left\{\Pr\left\{\mathbf{X}\to\hat{\mathbf{X}}\,|\mathbf{H}\right\}\right\}\\ &= \frac{1/12}{\det\left(\mathbf{I}_n+q_1\mathbf{K}\mathbf{A}\right)} + \frac{1/4}{\det\left(\mathbf{I}_n+q_2\mathbf{K}\mathbf{A}\right)},\end{aligned} \tag{23}$$

where $\mathbf{A} = \sum_{i=1}^{n}\left(\mathrm{diag}\{\mathbf{x}_i-\hat{\mathbf{x}}_i\}^H\mathrm{diag}\left\{\mathbf{x}_i-\hat{\mathbf{x}}_i\right\}\right)$, $\mathbf{K} = E\{\mathbf{h}\mathbf{h}^H\}$ is the covariance matrix of $\mathbf{H}$, $q_1 = 1/(2N_0)$ and $q_2 = 2/(3N_0)$. After obtaining the unconditional PEP, an upper bound on BER can be readily derived according to the union bounding technique as [43]

$$P_e \le \frac{1}{m2^m}\sum_{\mathbf{X}}\sum_{\hat{\mathbf{X}}\neq\mathbf{X}} N(\mathbf{X}\to\hat{\mathbf{X}})\Pr\left\{\mathbf{X}\to\hat{\mathbf{X}}\right\}, \tag{24}$$

where $N(\mathbf{X}\to\hat{\mathbf{X}})$ measures the number of bits in error between $\mathbf{X}$ and $\hat{\mathbf{X}}$.

From (24), the diversity order of our scheme is [23]

$$d_{min} = \min\mathrm{rank}\{\mathbf{K}\mathbf{A}\}. \tag{25}$$

Note that $\mathbf{K}$ becomes a diagonal matrix only and if only the subcarriers are independent. This can be guaranteed by interleaved grouping. Thus, the diversity order only depends on rank$\{\mathbf{A}\}$. Let E_1 denote the event that only the estimation of the index matrix is incorrect, E_2 denote the event that only the estimation of the modulated symbols is incorrect and E_3 denote the event that the estimations of both the index matrix and modulated symbols are incorrect. By definition, the rank of $\mathbf{A}$ can be calculated by

$$\min\mathrm{rank}\{\mathbf{A}\} = \begin{cases} 2 & E_1: \mathcal{J}_\alpha \neq \hat{\mathcal{J}}_\alpha,\ \mathbf{s}_\alpha = \hat{\mathbf{s}}_\alpha\\ n & E_2: \mathcal{J}_\alpha = \hat{\mathcal{J}}_\alpha,\ \mathbf{s}_\alpha \neq \hat{\mathbf{s}}_\alpha\\ 2 & E_3: \mathcal{J}_\alpha \neq \hat{\mathcal{J}}_\alpha,\ \mathbf{s}_\alpha \neq \hat{\mathbf{s}}_\alpha, \end{cases} \tag{26}$$

where $\hat{\mathcal{J}}_\alpha$ and $\hat{\mathbf{s}}_\alpha$ are estimations of $\mathcal{J}_\alpha$ and $\mathbf{s}_\alpha$, respectively. From (26), it can be seen that the diversity order of our scheme is two, which is higher than the unit diversity order of MM-OFDM-IM. This will be verified later in the simulation results.

B. DIVERSITY IMPROVING SCHEME

Rewriting $\mathbf{A} = \sum_{i=1}^{n}\left(\mathrm{diag}\{\mathbf{x}_i-\hat{\mathbf{x}}_i\}^H\mathrm{diag}\left\{\mathbf{x}_i-\hat{\mathbf{x}}_i\right\}\right)$ and referring to (25) and (26), it can be found that the error only caused by the modulated symbols ($\mathbf{s}_\alpha \neq \hat{\mathbf{s}}_\alpha$) leads to rank$\{\mathbf{A}\} = n$ while the error caused by the index matrix ($\mathcal{J}_\alpha \neq \hat{\mathcal{J}}_\alpha$) obtains rank$\{\mathbf{A}\} \ge 2$. Therefore, the overall diversity order of ST-MM-OFDM-IM is limited to two, which stems from the error event $\mathcal{J}_\alpha \neq \hat{\mathcal{J}}_\alpha$. According to this fact, we aim to increase the diversity up to n by appropriately enhancing the distance between the index matrices $\mathcal{J}_\alpha = \{\mathcal{J}_\alpha(1), \ldots, \mathcal{J}_\alpha(L_n)\}$.

In this paper, we utilize the computer search to find a new index matrix set achieving the diversity order of t

$$\mathcal{J}_\alpha^t = \{\mathcal{J}_\alpha(\omega_1), \ldots, \mathcal{J}_\alpha(\omega_{\kappa_t})\}, \tag{27}$$

where t represents the target diversity order with $2 < t \leq n$, κ_t is the number of $\mathcal{J}_\alpha^t$ and $\omega_i \in [1, 2, \ldots, L_n]$ is the selected index from $\mathcal{J}_\alpha$ with $i = 1, 2, \ldots, \kappa_t$. Any two index matrices in $\mathcal{J}_\alpha^t$ must satisfy the condition "rank$\{\mathbf{A}\} = t$", which guarantees the diversity order of t.

Taking $n = 4$ as an example, we have $L_4 = 576$. Randomly selecting 512 index matrices (Latin squares) with $p_1 = 9$ bits only obtains the diversity of two in ST-MM-OFDM-IM.

To increase the diversity order up to 4 ($t = 4$), we obtain a new set as

$$\begin{aligned}\mathcal{J}_\alpha^4 &= \{\mathcal{J}_\alpha(\omega_1), \ldots, \mathcal{J}_\alpha(\omega_{24})\} \\ &= \left\{\begin{bmatrix} 1 & 2 & 3 & 4 \\ 2 & 1 & 4 & 3 \\ 3 & 4 & 1 & 2 \\ 4 & 3 & 2 & 1 \end{bmatrix}, \ldots, \begin{bmatrix} 4 & 3 & 2 & 1 \\ 3 & 4 & 1 & 2 \\ 2 & 1 & 4 & 3 \\ 1 & 2 & 3 & 4 \end{bmatrix}\right\}.\end{aligned} \tag{28}$$

Note that there are 24 index matrices in $\mathcal{J}_\alpha^4$ ($\kappa_t = 24$). To modulate information bits, only 16 candidates are selected, which leads to $p_1 = 4$ bits. Moreover, in order to achieve a diversity order of 3 for $n = 4$, we obtain the resulting $\mathcal{J}_\alpha^3$ containing 5 candidates as

$$\begin{aligned}\mathcal{J}_\alpha^3 &= \{\mathcal{J}_\alpha(\omega_1), \ldots, \mathcal{J}_\alpha(\omega_5)\} \\ &= \left\{\begin{bmatrix} 1 & 2 & 3 & 4 \\ 2 & 1 & 4 & 3 \\ 3 & 4 & 1 & 2 \\ 4 & 3 & 2 & 1 \end{bmatrix}, \ldots, \begin{bmatrix} 1 & 2 & 3 & 4 \\ 3 & 4 & 1 & 2 \\ 2 & 3 & 4 & 1 \\ 4 & 1 & 2 & 3 \end{bmatrix}\right\}.\end{aligned} \tag{29}$$

With respect to $\mathcal{J}_\alpha^3$, 4 out of 5 candidates are used to map $p_1 = 2$ bits. Compared to the index bits of diversity order of 2, 7 and 5 index bits are reduced in the schemes of diversity orders of 3 and 4, respectively.

Accordingly, it can be found that the transmit diversity is expected to improve at the expense of the decreased index bits, which can be attributed to the trade-off between the diversity gain and multiplexing gain. It is worth noting that the index matrix set $\mathcal{J}_\alpha^t$ is not fixed that may be obtained as the different candidates by different searching methods.

V. SIMULATION RESULTS AND ANALYSIS

In this section, we conduct computer simulations to evaluate the BER performance of ST-MM-OFDM-IM systems under the assumption of Rayleigh fading channels and perfect channel estimation. For the sake of simplicity, we denote "MM-OFDM-IM (n, M), PSK/QAM" as the MM-OFDM-IM scheme with n subcarriers and n different M-ary PSK/QAM constellations, "ST-MM-OFDM-IM (n, M), PSK/QAM" as the ST-MM-OFDM-IM scheme with n subcarriers and n different M-ary PSK/QAM constellations in n time slots and "ST-MM-OFDM-IM (n, M), PSK/QAM, $D(\epsilon)$" as the diversity improvement scheme of "ST-MM-OFDM-IM (n, M), PSK/QAM" with diversity order of ϵ. Assume that the n different M-PSK constellations for ST-MM-OFDM-IM are set as the rotated PSK constellations with n rotated angles, which are given by "$n = 2$ with $\theta_1 = 0°, \theta_2 = 60°$", "$n = 3$ with $\theta_1 = 0°, \theta_2 = 30°, \theta_3 = 55°$" and "$n = 4$ with $\theta_1 = 0°, \theta_2 = 30°, \theta_3 = 55°, \theta_4 = 78°$".

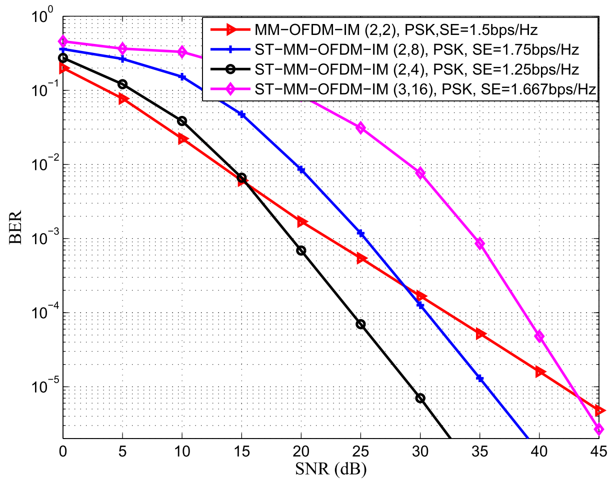

FIGURE 4. Comparison between ST-MM-OFDM-IM and MM-OFDM-IM.

We compare the BER performance of "ST-MM-OFDM-IM (2, 4), PSK", "ST-MM-OFDM-IM (2, 8), PSK", "ST-MM-OFDM-IM (3, 16), PSK" and "MM-OFDM-IM (2, 2), PSK" in Fig. 4. It can be seen that all curves with different configurations of ST-MM-OFDM-IM are better than that of the conventional MM-OFDM-IM scheme in the high SNR region. Specifically, compared to "MM-OFDM-IM (2, 2), PSK" with 1.5bps/Hz, "ST-MM-OFDM-IM (2, 2), PSK" with 1.25bps/Hz and "ST-MM-OFDM-IM (2, 8), PSK" with 1.75bps/Hz, both achieve the better performance at the SNR> 15dB and 29dB, respectively. At BER $= 10^{-3}$, it can be seen that "ST-MM-OFDM-IM (2, 2), PSK" with 1.25bps/Hz obtains an almost 4dB SNR gain compared with "MM-OFDM-IM (2, 2), PSK" with 1.5bps/Hz. Since the SE of "ST-MM-OFDM-IM (2, 2), PSK" is less than that of "MM-OFDM-IM (2, 2), PSK", it is hard to conclude that our proposed scheme outperforms the conventional MM-OFDM-IM scheme. However, at BER $= 10^{-4}$, the proposed scheme "ST-MM-OFDM-IM (2, 8), PSK" with a greater SE also achieves an about 1.5dB SNR gain with respect to "MM-OFDM-IM (2, 2), PSK". Accordingly, we finally find that the ST-MM-OFDM-IM scheme outperforms the conventional MM-OFDM-IM scheme. Additionally, we can see that "ST-MM-OFDM-IM (3, 16), PSK" with 1.667bps/Hz becomes better than "MM-OFDM-IM (2, 2), PSK", which further verifies our conclusion. Actually, this is because all ST-MM-OFDM-IM systems achieve the diversity order of two while MM-OFDM-IM systems obtain unit diversity

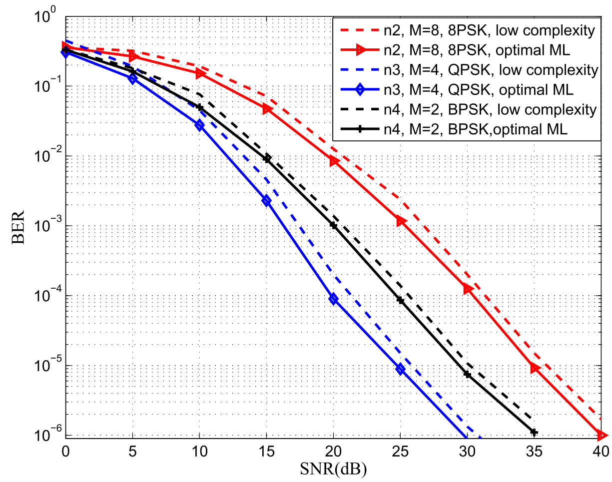

FIGURE 5. Performance of the low-complexity detection in ST-MM-OFDM-IM.

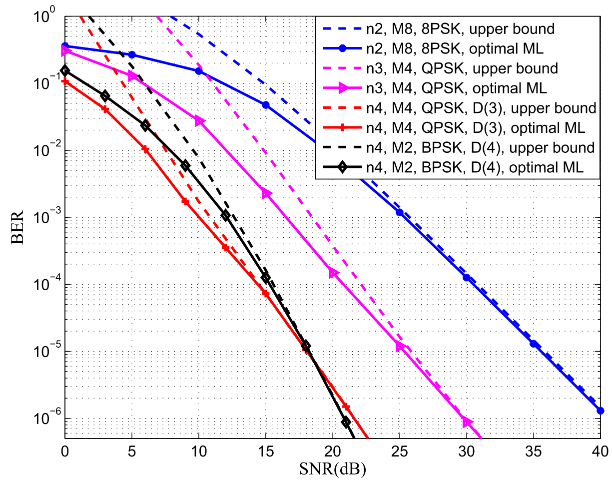

FIGURE 6. BER performance of ST-MM-OFDM-IM with different configurations.

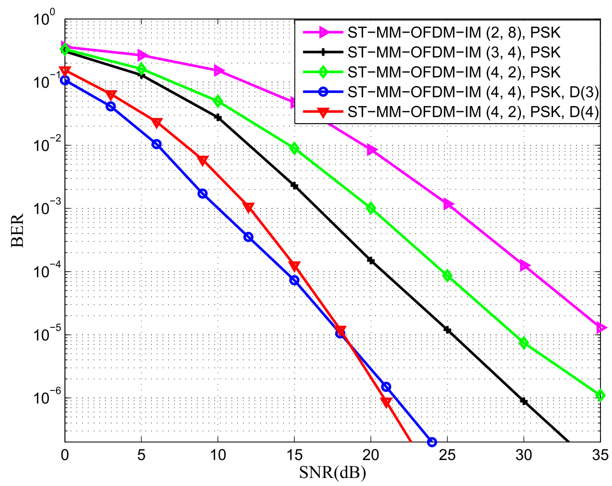

FIGURE 7. BER performance of ST-MM-OFDM-IM with different configurations.

order, which verifies the theoretical analysis in Section IV. On the other hand, we also find that increasing the number of subcarriers n does not change the diversity order. According to the diversity enhancement, it is worth noting that our proposed scheme still outperforms both the conventional OFDM-IM and OFDM schemes.

Fig. 5 presents the comparison results between the optimal ML detection and the proposed low-complexity detection for "ST-MM-OFDM-IM $(2, 8)$, PSK", "ST-MM-OFDM-IM $(3, 4)$, PSK" and "ST-MM-OFDM-IM $(4, 2)$, PSK". In Fig. 5, we can see that the proposed detection approaches the optimal ML detection with a small performance loss. Specifically, for the proposed scheme with $n = 4$ and $M = 2$, the low-complexity detection only has a less than 1dB performance gap in the high SNR region compared with the optimal ML detection. Besides, the proposed detection method in "ST-MM-OFDM-IM $(4, 2)$, PSK" also obtains about 1dB performance loss in the low SNT region, which makes our low-complexity detection more available through all SNRs. Similarly, the low-complexity detection for both "ST-MM-OFDM-IM $(2, 8)$, PSK" and "ST-MM-OFDM-IM $(3, 4)$, PSK" still exhibits a small and unchanged performance loss in the entire SNR region. It is worth noting that the small performance loss can be understood since the modulated symbols estimated in Step 1 are iteratively used for determining the row modes in other $(n - 1)$ detection steps, which easily occurs the chained detection error on the index matrix. However, the small performance loss is acceptable for the proposed low complexity detection.

Fig. 6 shows the BER performance for "ST-MM-OFDM-IM $(2, 8)$, PSK", "ST-MM-OFDM-IM $(3, 4)$, PSK", "ST-MM-OFDM-IM $(4, 4)$, PSK-D(3)" and "ST-MM-OFDM-IM $(4, 2)$, PSK-D(4)". From Fig. 6, it can be seen that the theoretical curves match the simulation results very well for all configurations in the high SNR region, which validates our analysis in Section IV. In addition, we can see that "ST-MM-OFDM-IM $(2, 8)$, PSK" with the SE of 1.75bps/Hz performs the worst and "ST-MM-OFDM-IM $(3, 4)$, PSK" with the SE of 1bps/Hz acquires a better performance. Importantly, due to the diversity improvement, both "ST-MM-OFDM-IM $(4, 4)$, PSK-D(3)" and "ST-MM-OFDM-IM $(4, 2)$, PSK-D(4)" achieve huge performance enhancements compared with "ST-MM-OFDM-IM $(2, 8)$, PSK" and "ST-MM-OFDM-IM $(3, 4)$, PSK".

To further evaluate the diversity improvement scheme, we compare the BER performance of "ST-MM-OFDM-IM $(2, 8)$, PSK", "ST-MM-OFDM-IM $(3, 4)$, PSK", "ST-MM-OFDM-IM $(4, 2)$, PSK", "ST-MM-OFDM-IM $(4, 4)$, PSK, D(3)" and "ST-MM-OFDM-IM $(4, 2)$, PSK, D(4)" in Fig. 7. From Fig. 7, it follows that the ST-MM-OFDM-IM schemes with $n = 2, 3$ and $M = 8, 4$ obtain the same diversity order of two. By resorting to the index matrix sets $\mathcal{J}_\alpha^3$ and $\mathcal{J}_\alpha^4$ in (29) and (28), respectively, we plot the BER performance of "ST-MM-OFDM-IM $(4, 4)$, PSK, D(3)" and "ST-MM-OFDM-IM $(4, 2)$, PSK, D(4)". For comparison, we also plot the BER performance of "ST-MM-OFDM-IM (4, 2), PSK" without taking into account the diversity improvement scheme, which utilizes all possible 576 index matrices of $\mathcal{J}_\alpha$. As seen from Fig. 7, "ST-MM-OFDM-IM (4, 2), PSK" achieves a diversity order of two, while "ST-MM-OFDM-IM (4, 4), PSK, D(3)" and "ST-MM-OFDM-IM (4, 2), PSK, D(4)" achieve diversity orders of 3 and 4, respectively. It can be also seen that although "ST-MM-OFDM-IM (4, 4), PSK, D(3)" with 0.625bps/Hz obtains a litter higher SE than "ST-MM-OFDM-IM (4, 2), PSK, D(4)" with 0.5bps/Hz, "ST-MM-OFDM-IM (4, 4), PSK, D(3)" still performs better than "ST-MM-OFDM-IM (4, 2), PSK, D(4)" in the low SNR region. This performance gain can be attributed to the fact that the BER is mainly determined by the error on index bits, where "ST-MM-OFDM-IM (4, 4), PSK, D(3)" has 2 of 10 index bits and "ST-MM-OFDM-IM (4, 2), PSK, D(4)" has 4 of 8 index bits. In the high SNR region, due to the diversity effect, "ST-MM-OFDM-IM (4, 2), PSK, D(4)" finally surpasses "ST-MM-OFDM-IM (4, 4), PSK, D(3)" when SNR goes to about 18dB. As revealed in Section IV, this diversity improvement comes at a price of loss of index bits.

VI. CONCLUSIONS

In this paper, we have proposed the ST-MM-OFDM-IM scheme, which merges the space time concept into MM-OFDM-IM, to increase the diversity order of MM-OFDM-IM up to two. Unlike MM-OFDM-IM, ST-MM-OFDM-IM transmits the signal matrix (n signal vectors of MM-OFDM-IM) over n time slots, where the index matrix of the signal matrix follows the rule of Latin square. A low-complexity detection method for ST-MM-OFDM-IM has been proposed to mitigate the burden of the optimal ML detection with a small and constant performance loss. An upper bound on the BER has also been studied. In addition, the diversity improving scheme of ST-MM-OFDM-IM has been proposed to achieve the full diversity order of n at the cost of SE. Simulation results have shown that the ST-MM-OFDM-IM scheme significantly outperforms the conventional MM-OFDM-IM scheme in the high SNR region and also shown that the diversity order of ST-MM-OFDM-IM can be improved to n by properly choosing the index matrices.

REFERENCES

[1] E. Basar, M. Wen, R. Mesleh, M. Di Renzo, Y. Xiao, and H. Haas, "Index modulation techniques for next-generation wireless networks," *IEEE Access*, vol. 5, pp. 16693–16746, 2017.

[2] M. Wen, X. Cheng, and L. Yang, *Index Modulation for 5G Wireless Communications*. Berlin, Germany: Springer, 2017.

[3] R. Y. Mesleh, H. Haas, S. Sinanovic, C. W. Ahn, and S. Yun, "Spatial modulation," *IEEE Trans. Veh. Technol.*, vol. 57, no. 4, pp. 2228–2241, Jul. 2008.

[4] R. Mesleh, O. Hiari, A. Younis, and S. Alouneh, "Transmitter design and hardware considerations for different space modulation techniques," *IEEE Trans. Wireless Commun.*, to be published.

[5] P. Yang, M. Di Renzo, Y. Xiao, S. Li, and L. Hanzo, "Design guidelines for spatial modulation," *IEEE Commun. Surveys Tuts.*, vol. 17, no. 1, pp. 6–26, 1st Quart., 2015.

[6] M. Di Renzo, H. Haas, and P. M. Grant, "Spatial modulation for multiple-antenna wireless systems: A survey," *IEEE Commun. Mag.*, vol. 49, no. 12, pp. 182–191, Dec. 2011.

[7] J. Jeganathan, A. Ghrayeb, L. Szczecinski, and A. Ceron, "Space shift keying modulation for MIMO channels," *IEEE Trans. Wireless Commun.*, vol. 8, no. 7, pp. 3692–3703, Jul. 2009.

[8] A. Younis, N. Serafimovski, R. Mesleh, and H. Haas, "Generalised spatial modulation," in *Proc. Conf. Rec. 44th Asilomar Conf. Signals, Syst. Comput.*, Pacific Grove, CA, USA, Nov. 2010, pp. 1498–1502.

[9] J. Jeganathan, A. Ghrayeb, and L. Szczecinski, "Generalized space shift keying modulation for MIMO channels," in *Proc. IEEE 19th Int. Symp. PIMRC*, Cannes, France, Sep. 2008, pp. 1–5.

[10] R. Mesleh, S. S. Ikki, and H. M. Aggoune, "Quadrature spatial modulation," *IEEE Trans. Veh. Technol.*, vol. 64, no. 6, pp. 2738–2742, Jun. 2015.

[11] R. Mesleh, S. Althunibat, and A. Younis, "Differential quadrature spatial modulation," *IEEE Trans. Commun.*, vol. 65, no. 9, pp. 3810–3817, Sep. 2017.

[12] S. Sugiura, S. Chen, and L. Hanzo, "Generalized space-time shift keying designed for flexible diversity-, multiplexing- and complexity-tradeoffs," *IEEE Trans. Wireless Commun.*, vol. 10, no. 4, pp. 1144–1153, Apr. 2011.

[13] E. Basar, U. Aygolu, E. Panayirci, and H. V. Poor, "Space-time block coded spatial modulation," *IEEE Trans. Commun.*, vol. 59, no. 3, pp. 823–832, Mar. 2011.

[14] B. Shamasundar, S. Jacob, S. Bhat, and A. Chockalingam, "Multidimensional index modulation in wireless communications," in *Proc. Inf. Theory Appl. Workshop (ITA)*, San Diego, CA, USA, Feb. 2017, pp. 1–10.

[15] Y. Bian, X. Cheng, M. Wen, L. Yang, H. V. Poor, and B. Jiao, "Differential spatial modulation," *IEEE Trans. Veh. Technol.*, vol. 64, no. 7, pp. 3262–3268, Jul. 2015.

[16] J. Li, M. Wen, X. Cheng, Y. Yan, S. Song, and M. H. Lee, "Differential spatial modulation with Gray coded antenna activation order," *IEEE Commun. Lett.*, vol. 20, no. 6, pp. 1100–1103, Jun. 2016.

[17] L.-L. Yang, "Transmitter preprocessing aided spatial modulation for multiple-input multiple-output systems," in *Proc. 73rd IEEE Veh. Techn. Conf. (VTC Spring)*, Budapest, Hungary, May 2011, pp. 1–5.

[18] R. Zhang, L. Yang, and L. Hanzo, "Generalised pre-coding aided spatial modulation," *IEEE Trans. Wireless Commun.*, vol. 12, no. 11, pp. 5434–5443, Nov. 2013.

[19] A. Stavridis *et al.*, "Performance analysis of multi-stream receive spatial modulation in the MIMO broadcast channel," *IEEE Trans. Wireless Commun.*, vol. 15, no. 3, pp. 1808–1820, Mar. 2016.

[20] J. Li, M. Wen, X. Cheng, Y. Yan, S. Song, and M. H. Lee, "Generalized precoding-aided quadrature spatial modulation," *IEEE Trans. Veh. Technol.*, vol. 66, no. 2, pp. 1881–1886, Feb. 2017.

[21] R. Abu-Alhiga and H. Haas, "Subcarrier-index modulation OFDM," in *Proc. IEEE 20th Int. Symp. Pers., Indoor Mobile Radio Commun. (PIMRC)*, Tokyo, Japan, Sep. 2009, pp. 177–181.

[22] D. Tsonev, S. Sinanovic, and H. Haas, "Enhanced subcarrier index modulation (SIM) OFDM," in *Proc. IEEE Global Commun. Conf. (GLOBECOM) Workshops*, Houston, TX, USA, Dec. 2011, pp. 728–732.

[23] E. Basar, U. Aygolu, E. Panayirci, and H. V. Poor, "Orthogonal frequency division multiplexing with index modulation," *IEEE Trans. Signal Process.*, vol. 61, no. 22, pp. 5536–5549, Nov. 2013.

[24] M. Wen, Y. Zhang, J. Li, E. Basar, and F. Chen, "Equiprobable subcarrier activation method for OFDM with index modulation," *IEEE Commun. Lett.*, vol. 20, no. 12, pp. 2386–2389, Dec. 2016.

[25] Y. Xiao, S. Wang, L. Dan, X. Lei, P. Yang, and W. Xiang, "OFDM with interleaved subcarrier-index modulation," *IEEE Commun. Lett.*, vol. 18, no. 8, pp. 1447–1450, Aug. 2014.

[26] M. Wen, X. Cheng, M. Ma, B. Jiao, and H. V. Poor, "On the achievable rate of OFDM with index modulation," *IEEE Trans. Signal Process.*, vol. 64, no. 8, pp. 1919–1932, Apr. 2016.

[27] Q. Ma, Y. Xiao, L. Dan, P. Yang, L. Peng, and S. Li, "Subcarrier allocation for OFDM with index modulation," *IEEE Commun. Lett.*, vol. 20, no. 7, pp. 1469–1472, Jul. 2016.

[28] A. I. Siddiq, "Low complexity OFDM-IM detector by encoding all possible subcarrier activation patterns," *IEEE Commun. Lett.*, vol. 20, no. 3, pp. 446–449, Mar. 2016.

[29] E. Basar, "OFDM with index modulation using coordinate interleaving," *IEEE Wireless Commun. Lett.*, vol. 4, no. 4, pp. 381–384, Aug. 2015.

[30] M. Wen, X. Cheng, L. Yang, Y. Li, X. Cheng, and F. Ji, "Index modulated OFDM for underwater acoustic communications," *IEEE Commun. Mag.*, vol. 54, no. 5, pp. 132–137, May 2016.

[31] E. Başar, E. Panayirci, M. Uysal, and H. Haas, "Generalized LED index modulation optical OFDM for MIMO visible light communications systems," in *Proc. IEEE Int. Conf. Commun. (ICC)*, Kuala Lumpur, Malaysia, May 2016, pp. 1–5.
[32] R. Fan, Y. J. Yu, and Y. L. Guan, "Generalization of orthogonal frequency division multiplexing with index modulation," *IEEE Trans. Wireless Commun.*, vol. 14, no. 10, pp. 5350–5359, Oct. 2015.
[33] E. Basar, "On multiple-input multiple-output OFDM with index modulation for next generation wireless networks," *IEEE Trans. Signal Process.*, vol. 64, no. 15, pp. 3868–3878, Aug. 2016.
[34] J. Crawford, E. Chatziantoniou, and Y. Ko, "On the SEP analysis of OFDM index modulation with hybrid low complexity greedy detection and diversity reception," *IEEE Trans. Veh. Technol.*, vol. 66, no. 9, pp. 8103–8118, Sep. 2017.
[35] B. Zheng, F. Chen, M. Wen, F. Ji, H. Yu, and Y. Liu, "Low complexity ML detector and performance analysis for OFDM with in-phase/quadrature index modulation," *IEEE Commun. Lett.*, vol. 19, no. 11, pp. 1893–1896, Nov. 2015.
[36] B. Zheng, M. Wen, E. Basar, and F. Chen, "Multiple-input multiple-output OFDM with index modulation: Low-complexity detector design," *IEEE Trans. Signal Process.*, vol. 65, no. 11, pp. 2758–2772, Jun. 2017.
[37] T. Mao, Z. Wang, Q. Wang, S. Chen, and L. Hanzo, "Dual-mode index modulation aided OFDM," *IEEE Access*, vol. 5, pp. 50–60, 2017.
[38] T. Mao, Q. Wang, and Z. Wang, "Generalized dual-mode index modulation aided OFDM," *IEEE Commun. Lett.*, vol. 21, no. 4, pp. 761–764, Apr. 2017.
[39] M. Wen, E. Basar, Q. Li, B. Zheng, and M. Zhang, "Multiple-mode orthogonal frequency division multiplexing with index modulation," *IEEE Trans. Commun.*, vol. 65, no. 9, pp. 3892–3906, Sep. 2017.
[40] M. Simon and M. S. Alaouni, *Digital Communications over Fading Channels*. Hoboken, NJ, USA: Wiley, 2005.
[41] W. J. Dixon and F. J. Massey, *Introduction to Statistical Analysis*, 1st ed. New York, NY, USA: McGraw-Hill, 1951.
[42] M. Chiani and D. Dardari, "Improved exponential bounds and approximation for the Q-function with application to average error probability computation," in *Proc. IEEE Global Telecommun. Conf.*, Bologna, Italy, Nov. 2002, pp. 1399–1402.
[43] J. G. Proakis, *Digital Communications*, 3rd ed. New York, NY, USA: McGraw-Hill, 1995.

JUN LI (S'13–M'17) received the M.S. and the Ph.D. degrees from Chonbuk National University, Jeonju, South Korea, in 2011 and 2017, respectively. He has been an Assistant Professor with Guangzhou University, Guangzhou, China. He had participated as the Vice Head Researcher in the World Class University Project, sponsored by the National Research Foundation of Korea Grant funded by the Korean Ministry of Education Science and Technology. His research interests include spatial modulation and OFDM index modulation.

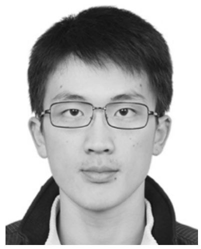

MIAOWEN WEN (M'14) received the B.S. degree from Beijing Jiaotong University, Beijing, China, in 2009, and the Ph.D. degree from Peking University, Beijing, China, in 2014. From 2012 to 2013, he was a Visiting Student Research Collaborator with Princeton University, Princeton, NJ, USA. He is currently an Associate Professor with the South China University of Technology, Guangzhou, China. He has authored a book and over 70 papers in refereed journals and conference proceedings. His research interests include index modulation and nonorthogonal multiple access techniques.

Dr. Wen received the Best Paper Award from the IEEE International Conference on Intelligent Transportation Systems Telecommunications in 2012, the IEEE International Conference on Intelligent Transportation Systems in 2014, and the IEEE International Conference on Computing, Networking and Communications in 2016. He received the Excellent Doctoral Dissertation Award from Peking University. He currently serves as an Associate Editor of the IEEE ACCESS, and on the Editorial Board of the *EURASIP Journal on Wireless Communications and Networking* and the *ETRI Journal*.

XUEQIN JIANG (M'12) received the B.S degree in computer science from the Nanjing Institute of Technology, Nanjing, Jiangsu, China, the M.S and Ph.D. degrees in electronics engineering from Chonbuk National University, Jeonju, South Korea. He is currently an Associate Professor with the School of Information Science and Technology, Donghua University, Shanghai, China. He has authored/co-authored over 70 technical papers, several book chapters. His main research interests include LDPC codes, physical-layer security, and wireless communications.

WEI DUAN received the B.S. degree from the Chengdu University of Technology, Chengdu, China, in 2008, the M.S. and Ph.D. degrees from Chonbuk National University, Jeonju, South Korea, in 2012 and 2017, respectively. He is currently a Lecturer with Nantong University, Nantong, China. His research interests include cooperative networks and non-orthogonal multiple access techniques.